Draft version March 7, 2023
Typeset using LaTeX twocolumn style in AASTeX63

arXiv:2303.03192v1 [astro-ph.IM] 6 Mar 2023

Deep symbolic regression for physics guided by units constraints: toward the automated discovery of physical laws

Wassim Tenachi,[1] Rodrigo Ibata,[1] and Foivos I. Diakogiannis[2]

[1] Université de Strasbourg, CNRS, Observatoire astronomique de Strasbourg, UMR 7550, F-67000 Strasbourg, France
[2] Data61, CSIRO, Kensington, WA 6155, Australia

(Received March 03, 2023)

Submitted to ApJ

ABSTRACT

Symbolic Regression is the study of algorithms that automate the search for analytic expressions that fit data. While recent advances in deep learning have generated renewed interest in such approaches, efforts have not been focused on physics, where we have important additional constraints due to the units associated with our data. Here we present Φ-SO, a Physical Symbolic Optimization framework for recovering analytical symbolic expressions from physics data using deep reinforcement learning techniques by learning units constraints. Our system is built, from the ground up, to propose solutions where the physical units are consistent by construction. This is useful not only in eliminating physically impossible solutions, but because it restricts enormously the freedom of the equation generator, thus vastly improving performance. The algorithm can be used to fit noiseless data, which can be useful for instance when attempting to derive an analytical property of a physical model, and it can also be used to obtain analytical approximations to noisy data. We showcase our machinery on a panel of examples from astrophysics.

Keywords: Neural networks (1933), Regression (1914), Astronomy data modeling (1859)

1. INTRODUCTION

Galileo famously intuited in Opere Il Saggiatore (Galilei 1623) that the book of the Universe "è scritto in lingua matematica". Ever since, it has been a central concern of physics to attempt to explain the properties of nature in mathematical terms, by proposing or deriving mathematical expressions that encapsulate our measurements from experiment and observation. This approach has proven to be immensely powerful. Through trial and error over the centuries, the great masters of physics have developed and bequeathed us a rich toolbox of techniques that have allowed us to understand the world and build our modern technological civilization. But now, thanks to the development of modern deep learning networks, there is hope that this endeavor could be accelerated, by making use of the fact that machines are able to survey a vastly larger space of trial solutions than an unaided human.

Of course, since the beginning of the computer revolution, many methods have been developed to fit coefficients of linear or non-linear functions to data (see, e.g., Press et al. 2007). While such approaches are undoubtedly very useful, the procedures we wish to discuss in the present contribution are more general, in the sense that they aim to find the functions themselves, as well as any necessary fitting coefficients. In particular, we wish to infer a free-form symbolic analytical function $f : \mathbb{R}^n \longrightarrow \mathbb{R}$ that fits $y = f(\mathbf{x})$ given $(\mathbf{x}, y)$ data. In computer science, these procedures are generally referred to as "Symbolic Regression" (SR).

1.1. *Motivations from physics and Big Data*

Although there are multiple demonstrations of the capabilities of SR in physics (e.g., Wu & Tegmark 2019; Liu & Tegmark 2021; Liu et al. 2021; Lemos et al. 2022; DiPietro & Zhu 2022; Bartlett et al. 2022; Reinbold et al. 2021) and astrophysics (e.g., Wadekar et al. 2022; Matchev et al. 2022; Shao et al. 2022; Delgado et al. 2022; Wong & Cranmer 2022; Wadekar et al. 2020; Desmond et al. 2023), to date, symbolic regression has never been used to discover new physical laws from astrophysical measurements. Yet this may change thanks to new observational missions and surveys such as Gaia (Gaia Collaboration et al. 2016), Euclid (Laureijs et al. 2011), LSST (Ivezić et al. 2019; LSST Science Collabo-

ration et al. 2009) and SKA (Carilli & Rawlings 2004). With these and other large surveys, our field is entering a new era of data abundance, and there is considerable excitement at the possibility of discovering new physics from these unprecedentedly rich datasets. However, the colossal amount of data also presents significant conceptual challenges. Although deep learning will allow us to extract valuable information from the large surveys, it is both blessed and plagued by the underlying neural networks that are one of its most potent components. Neural networks are flexible and powerful enough to model any physical system (that can be described as a Lebesgue integrable function Lu et al. 2017) and work in high dimensions, but they unfortunately largely consist of non-interpretable black boxes. Clearly, interpretability and intelligibility are of great importance in physics, which begs the question: how can one harness information from these large datasets while retaining their ability to interpret? After training a deep neural network to fit a dataset, can one open the black box, to understand the physics modelled inside?

1.2. *Symbolic regression*

Symbolic regression addresses these issues by producing compact, interpretable and generalizable models. Indeed, the goal is to find very simple prescriptions such as Newton's law of universal gravitation that can explain well a vast number of experiments and observations. There are many advantages to discovering physical laws in the form of succinct mathematical expressions rather than large numerical models:

- Compactness: The models produced by SR are extremely compact compared to most numerical models. This makes the models computationally inexpensive to run and in principle also enables SR to correctly recover the exact underlying mathematical expression of a dataset using much less data than traditional machine learning approaches and with a robustness towards noise even for perfect model recovery (Wilstrup & Kasak 2021; Reinbold et al. 2021; La Cava et al. 2021).

- Generalization: In addition, the expressions produced by symbolic regression are less prone to overfitting on measurement errors and are much more robust and reliable outside of the fitting range provided by the data than large numerical models, showing overall much better generalization capabilities (Wilstrup & Kasak 2021) (we will provide an example of this in Section 5). This makes SR a potentially powerful tool to discover the most concise and general representation of the measurements.

- Intelligibility & interpretability: Since the models produced by SR consist of mathematical expressions, their behavior is intelligible to us, contrary to the case of large numerical models. This is of enormous value in physics (Wu & Tegmark 2019) as SR models may enable one to connect newly discovered physical laws with theory and make subsequent theoretical developments. More broadly, this approach fits into the increasing push towards intelligible (Sabbatini & Calegari 2022), explainable (Arrieta et al. 2020) and interpretable (Murdoch et al. 2019) machine learning models, which is especially important in fields where such models can affect human lives (European Commission 2021; 117th US Congress 2022).

However, although the prospect of using SR for discovering new physical laws may be very appealing, it is also extremely challenging to implement. It is useful to consider the difficulty of this problem if one were to approach it in a naive way. Suppose in the trial analytic expressions, we allow for an expression length of 30 symbols (as we will do below), and that there are 15 different variables or operations (e.g. x, $+$, $-$, $\times$, $/$, sin, log, ...) to chose from for each symbol. A naive brute-force attempt to fit the dataset might then have to consider up to $15^{30} \approx 1.9 \times 10^{35}$ trial solutions which is obviously vastly beyond our computational means to test against the data at the present day or at any time in the foreseeable future. This consideration does not even account for the optimization of free constants, which makes SR an "NP hard" (nondeterministic polynomial time) problem (Virgolin & Pissis 2022). The obvious conclusion one draws from these considerations is that symbolic regression requires one to develop highly efficient strategies to prune poor guesses.

1.3. *Physical Symbolic Regression*

There are multiple approaches to SR (detailed in Section 2) which are capable of generating accurate analytical models. However, in the context of physics, we have the additional requirement that our equations must be balanced in terms of their physical units, as otherwise the equation is simply non-sensical, irrespective of whether it gives a good fit to the numerical values of the data. Although powerful, to the best of our knowledge, all of the available SR approaches spend most of their time exploring a search space where the immense majority of candidate expressions are unphysical in terms of units and thus often end up producing unphysical models. A very simple solution to this problem would have been to use an existing SR code, and check *post hoc* whether the proposed solutions obey that constraint.

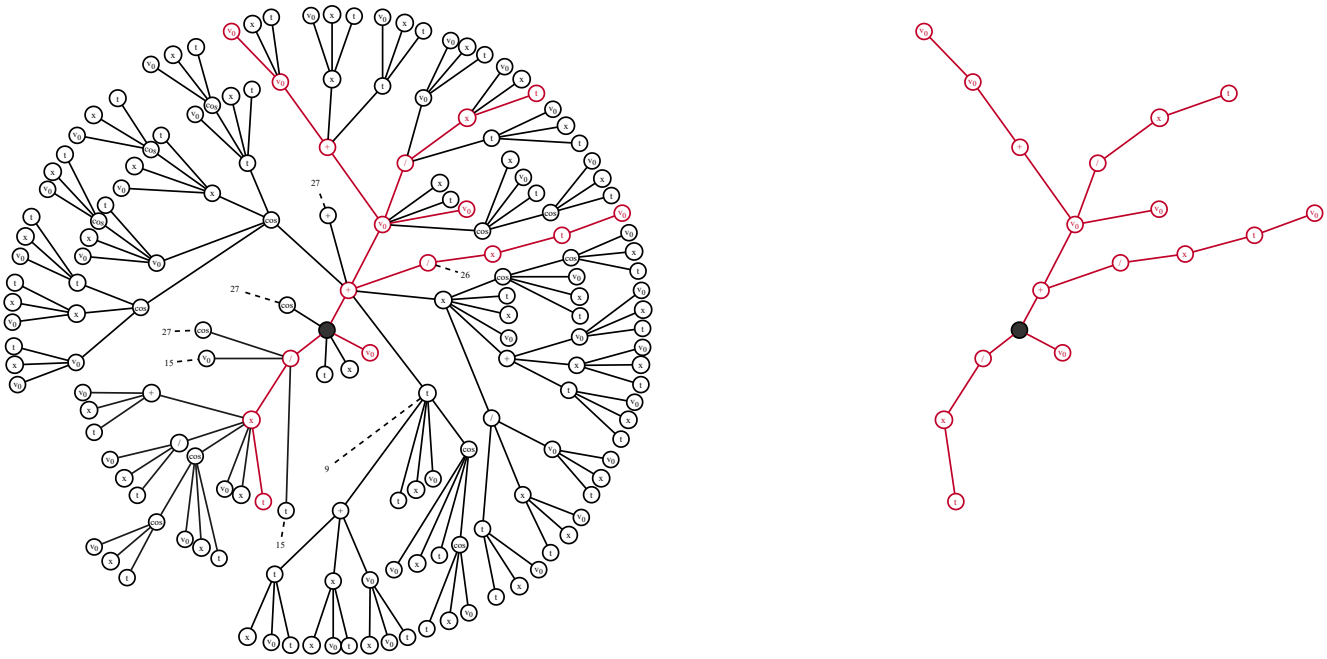

Search space

Search space with our *in situ* physical units prior

Figure 1. Illustration of the symbolic expression search space reduction enabled by our *in situ* physical units prior. We represent paths (in prefix notations) leading to expressions with physically-possible units (in red) and a small sample of the paths that lead to expressions with unphysical units (in black). Here we consider the recovery of a velocity v using a library of symbols $\{+, /, \cos, v_0, x, t\}$ where v_0 is a velocity, x is a length, and t is a time (limiting ourselves to 5 symbol long expressions for readability). This reduces the search space from 268 expressions to only 6.

But not only does that constitute an immense waste of time and computing resources, which could render many interesting SR tasks impossible, it also makes a significant fraction of the resulting "best" analytical models unusable and uninterpretable.

At first glance, one could think of the units constraints as severe restrictions that limit the capabilities of SR. However, in this work we show that respecting physical constraints actually helps improve SR performance not only in terms of interpretability but also in accuracy by guiding the exploration of the space of solutions towards exact analytical laws. This is consistent with the studies of Petersen et al. (2019, 2021); Kammerer et al. (2020) who found that using *in situ* constraints during analytical expression generation is much more efficient as it vastly reduces the search space of trial expressions (though we note their machinery is not capable of incorporating units constraints as it requires one to compute and exploit the whole graph describing an expression as a relational tree).

Here we present our physical symbolic optimization framework (Φ-SO) which was built from the ground up to incorporate and take full advantage of physical units information during symbolic regression. This addresses in part the combinatorial challenge discussed above in subsection 1.2. Our Φ-SO framework includes the units constraints *in situ* during the equation generation process, such that only equations with balanced units are proposed *by construction*, thus also greatly reducing the search space as illustrated in Figure 1.

Although our framework could be applied to virtually any one of the SR approaches described in Section 2, we chose to implement our algorithm in *pytorch* (Paszke et al. 2019, currently the most popular deep learning library) building upon key strategies pioneered in the state-of-the-art Deep Symbolic Regression framework proposed in Petersen et al. (2019) and Landajuela et al. (2021a) which relies on reinforcement learning via a risk-seeking policy gradient.

In the present study, we develop a foundational symbolic embedding for physics that enables the entire expression tree graph to be tackled, as well as local units constraints. This approach allows us to anticipate the required units for the subsequent symbol to be generated in a partially composed mathematical expression. By adopting this approach, we not only focus on training a neural network to generate increasingly precise expressions, as in Petersen et al. (2019), but we also generate

labels of the necessary units and actively train our neural network to adhere to such constraints. In essence, our method equips the neural network with the ability to learn to select the appropriate symbol in line with local units constraints.

To the best of our knowledge such a framework was never built before. This constitutes a first step in our planned research program of building a powerful general-purpose symbolic regression algorithm for astrophysics and other physical sciences. Our aim here is to present the algorithm to the community, show its workings and its potential, while leaving concrete astrophysical research applications to future studies.

The layout of this study is as follows. We first provide a brief overview of the recent SR literature in Section 2. Our Φ-SO framework is described in detail in Section 3, its capabilities are showcased on a panel of astrophysical test cases presented in Section 4, with results given in Section 5, and finally in Sections 6 and 7 we discuss the results and draw our conclusions.

2. RELATED WORKS – A BRIEF SURVEY OF MODERN SYMBOLIC REGRESSION

SR has traditionally been tackled using genetic algorithms where a population of candidate mathematical expressions are iteratively improved through operations inspired by natural evolution such as natural selection, crossover, and mutation. This type of approach includes the well known Eureqa software (Schmidt & Lipson 2009) (see Graham et al. 2013 for a benchmark of Eureqa's capabilities on astrophysical test cases), as well as more recent works (Cranmer 2020; Virgolin & Bosman 2022; Stephens 2015; Kommenda et al. 2020; Keren et al. 2023). In addition, SR has been implemented using various methods ranging from brute force to (un-)guided Monte-Carlo, all the way to probabilistic searches (McConaghy 2011; Kammerer et al. 2020; Bartlett et al. 2022; Brence et al. 2021; Jin et al. 2019), as well as through problem simplification algorithms (Luo et al. 2017; Tohme et al. 2022).

Given the great successes of deep learning techniques in many other fields, it is not surprising that they have now been applied to symbolic regression, and now challenge the reign of Eureqa-type approaches (La Cava et al. 2021; Matsubara et al. 2022). Multiple methods for incorporating neural networks into SR have been developed, ranging from powerful problem simplification schemes (Udrescu & Tegmark 2020; Udrescu et al. 2020; Cranmer et al. 2020; Keren et al. 2023), to end-to-end symbolic regression methods where a neural network is trained in a supervised manner to map the relationship between datasets and their corresponding symbolic functions (Kamienny et al. 2022; Vastl et al. 2022; d'Ascoli et al. 2022; Becker et al. 2022; Biggio et al. 2020; Alnuqaydan et al. 2022; Aréchiga et al. 2021), all the way to incorporating symbols into neural networks in place of activation functions to enable interpretability or to recover a mathematical expression (Martius & Lampert 2016; Zheng et al. 2022; Sahoo et al. 2018; Valle & Haddadin 2021; Kim et al. 2020; Panju & Ghodsi 2020). See La Cava et al. (2021) & Makke & Chawla (2022) for recent reviews of symbolic regression algorithms.

While some of the aforementioned algorithms excel at generating very accurate symbolic approximations, the reinforcement learning based deep symbolic regression framework proposed in Petersen et al. (2019) is the new standard for exact symbolic function recovery, particularly in the presence of noise (La Cava et al. 2021; Matsubara et al. 2022). This has resulted in a number of studies in the literature built on this framework (e.g., Du et al. 2022; DiPietro & Zhu 2022; Zheng et al. 2022; Landajuela et al. 2021b; Usama & Lee 2022).

3. METHOD

Considering the success of deep reinforcement learning methods in accurately recovering exact symbolic expressions, which is particularly important in the field of physics where precise physical law recovery is crucial, we have chosen to incorporate this methodology into the machine learning component of our physical symbolic regression approach. In Subsection 3.1, we describe how we generate analytical expressions from a recurrent neural network (RNN). Subsection 3.2 provides details about the algorithm we use to generate *in situ* units constraints, which are used to teach the RNN units rules and help to reduce the search space. And finally, in Subsection 3.3, we describe the reinforcement learning strategy we adopted to make our RNN not only produce accurate expressions but also physically meaningful ones.

3.1. *Generating symbolic expressions*

Symbolic expressions can be regarded as binary trees where each node represents a symbol of the expression in the library of available symbols, i.e., an input variable (e.g., x, t), a constant (e.g., v_0) or an operation (e.g., $+$, $-$, $\times$, $/$, sin, log, ...). In this representation, input variables and constants can be referred to as terminal nodes or symbols (having no child node), operations taking a single argument (e.g., sin, log, ...) are unary symbols (having one child node) and operations taking two arguments (e.g., $+$, $-$, $\times$, $/$, ...) are binary symbols. By considering each node first in depth and then left to right, one can compute a one dimensional list i.e.

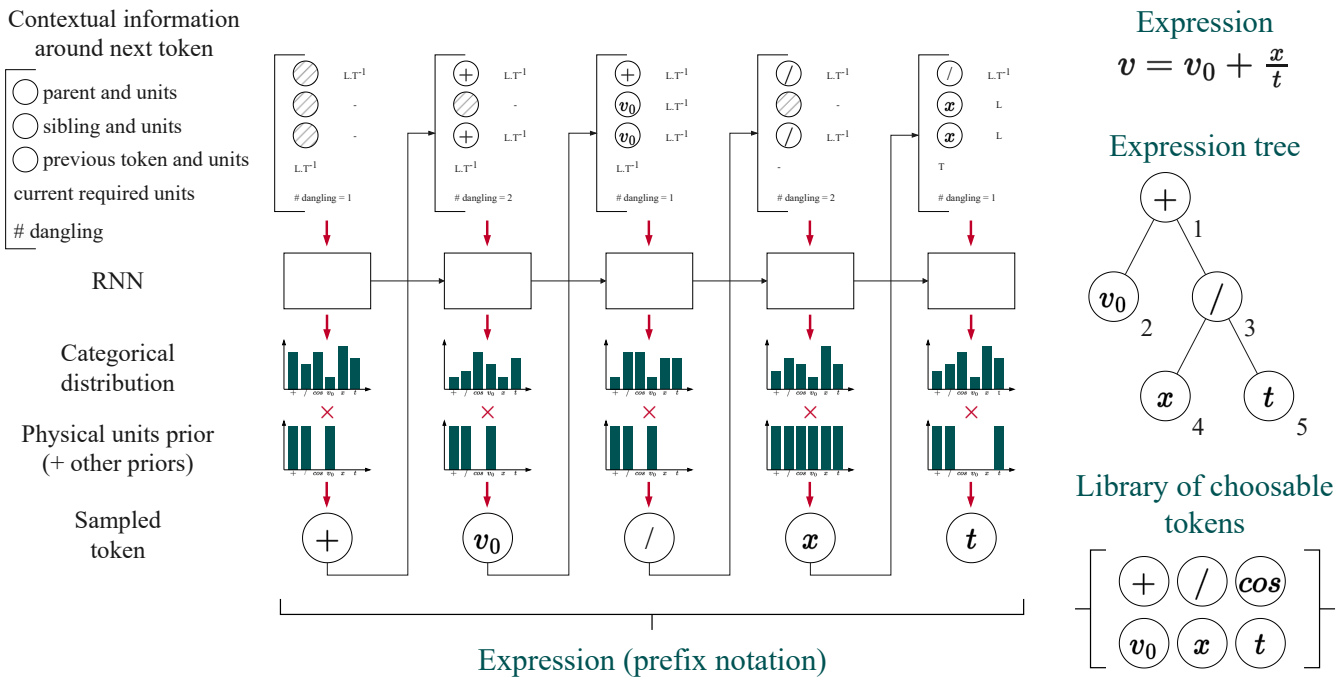

Figure 2. Expression generation sketch. The process starts at the top left RNN block. For each token, the RNN is given the contextual information regarding the surroundings of the next token to generate, namely: the parent, sibling and previously sampled token along with their units, the required units for the token to be generated and the dangling number (i.e. the minimum number of tokens needed to obtain a valid expression). Based on this information, the RNN produces a categorical distribution over the library of available tokens (top histograms) as well as a state which is transmitted to the RNN on its next call. The generated distribution is then masked based on local units constraints (bottom histograms), forbidding tokens that would lead to nonsensical expressions. The resulting token is sampled from this distribution, leading to the token '+' in this example. Repeating this process, from left to right, allows one to generate a complete physical expression, here $[+, v_0, /, x, t]$ which translates into $v_0 + x/t$ in the infix notation we are more familiar with.

a prefix[1] notation in which operators are placed before the corresponding operands in the expression, alleviating the need for parentheses. Using the prefix notation and treating symbols, referred to as tokens, as categories allows us to treat any expression as a mere sequence of categorical vectors. E.g., considering short toy library of tokens $\{+, \cos, x\}$, the operator $+$ can be encoded as $[1, 0, 0]$, the function cos as $[0, 1, 0]$ and the variable x as $[0, 0, 1]$.

As in previous deep symbolic regression studies (e.g., (Kamienny et al. 2022; Vastl et al. 2022; Petersen et al. 2019; Du et al. 2022; DiPietro & Zhu 2022), treating mathematical expressions as sequences allows us to employ traditional natural language processing techniques to sample them. Token sequences are generated by using an RNN, which, in a nutshell, is a neural network that can be called multiple times $i < N$ to generate a time dependent output as well as a time dependent S_i memory state. The RNN takes as input some time dependent observations O_i as well as the state of the previous call S_{i-1}. In practice, we use the RNN to generate a categorical probability distribution over the library of available tokens, which we then simply sample to draw a definite token. Once a token is generated, we feed its properties and the properties of its surroundings as observations for the next RNN call. We also feed as observations the minimum number of tokens still needed to obtain a valid analytical expression (i.e. the number of dangling nodes), the nature of the token which was sampled at the previous step, the sibling and parent tokens of the token to be generated in a tree representation, to which in the context of our Φ-SO framework we add the physical units of all of these tokens and the units required for the token to be generated so as to respect the units rules. This allows the inner mechanisms of the neural network to take into account not only the local structure of the expression for generating the next token, but also to take into account the local units constraints. The

[1] This is also called "Polish" notation, and can be converted to a tree representation or the "infix" notation which we are more familiar with, as there is a one-to-one relationship between them.

process described above can be repeated multiple times until a whole token function is generated in prefix notation, as illustrated in Figure 2.

It is important to note here that one can artificially tune the generated categorical distribution to incorporate prior knowledge *in situ* while expressions are being generated. One can for example zero-out the probability of some token depending on the context encoded in the expression tree being generated, thus greatly reducing search space (Petersen et al. 2019, 2021). We therefore adopt priors that force expressions sizes to be < 30 tokens long, to contain no more than 2 levels of nested trigonometric operations (e.g., forbidding $\cos(f.t + \sin(x/x0 + \tan(\square)))$ but still allowing $\cos(f.t+\sin(x/x0)))$, contain no self nesting of exponent and log operators (e.g., forbidding $e^{e^{\square}}$) and forbid useless inverse unary operations (e.g., forbidding $e^{\log \square}$). It is worth noting that the combination of priors we employ can conflict in some cases, in which case we discard the resulting candidate.

In addition to the above priors whose formulation depends on the local tree structure (parent, sibling, ancestors), we are able to create priors that take into account the entire tree structure. This is rendered possible by the fact that contrary to most other SR algorithms (including the state-of-the-art Deep Symbolic Regression Petersen et al. 2019), in the Φ-SO framework we compute and keep track of the full graph of the tree representation while the expression is being generated, as it is an essential ingredient to compute units constraints as detailed in the following subsection.

3.2. *In situ physical units constraints*

As discussed above, in physics we already know that some combinations of tokens are not possible due to units constraints. For example, if the algorithm is in the process of generating an expression in which a velocity (v_0) is summed with a length (x) divided by a token or sub-expression which is still to be generated ($\square$):

$$v_0 + \frac{x}{\square}\,, \tag{1}$$

then based on the expression tree (as shown in Figure 2), we already know that that $\square$ must be a time variable or a more complicated sub-tree that eventually ends up having units of time, but that it is definitely not a length or a dimensionless operator such as the log function.

Computing such constraints *in situ* i.e. in incomplete, only partially sampled trees (containing empty placeholder nodes) is much harder than simply checking *post hoc* if the units of a given equation make sense, because in some situations it is impossible to compute such constraints until later on in the sequence, leaving the units of some nodes *free* (i.e. compatible with any units at this point in the sequence). For example, it is impossible to compute the units requirement in the left child node of a (binary) multiplication operator token $\square \times \triangle$, as any units in the $\square$ left child node could be compensated by units in the $\triangle$ right child node. Algorithm 1 shows the pseudo-code of the procedure we devised to compute the required units whenever possible and leaving them as *free* otherwise. The procedure is applied to a token at position $i < N$ in an incomplete sequence of tokens $\{\tau_j\}_{j<N}$ of size N, knowing the units of terminal nodes and of the root node (e.g., respectively $\{v_0, x, t\}$ and $\{v\}$ in the example of Figure 2). The sequence may be partially made up of placeholder tokens of yet undetermined nature (representing dangling nodes). Running algorithm 1 before each token generation step allows one to have a maximally informed expression tree graph in terms of units.

Having access *in situ* to the (required) physical units of tokens allows us to not only to inform the neural network of our expectations in terms of units as well as to feed it units of surrounding tokens, thus allowing the model to leverage such information, but also to express a prior distribution over the library. This enables the algorithm to zero-out the probability of forbidden symbols that would result in expressions that violate units rules. Combining this prior distribution with the categorical distribution given by the RNN while expressions are being generated results in a system where *by construction* only correct expressions with correct physical units can be formulated and learned on by the neural network.

3.3. *Learning*

One might naively imagine that symbolic regression problems could be solved by directly optimizing the choice of symbols to fit the problem, using the auto-differentiation capabilities of modern machine learning frameworks[2]. Unfortunately this approach cannot be used for symbolic regression because the cost function is non differentiable (the choice of selecting say the sin function over log is not differentiable with respect to the data), which prevents one from using gradient descent. A practical solution is to use a neural network as a "middle man" to generate a categorical distribution from which we can sample symbols. One can then optimize the parameters of this neural network whose task

[2] Most machine learning tasks use the differentiability of the implemented model with respect to the data to implement a (stochastic) gradient descent towards an optimal model solution that fits the data best

Algorithm 1: *In situ* units requirements algorithm.

Input: (In)-complete expression $\{\tau_j\}_{j<N}$, Position of token i
Output: Required physical units Φ_i of token at i

function ComputeRequiredUnits($\{\tau_j\}_{j<N}, i$)
  $p \leftarrow$ PositionOfParent(i)
  $s \leftarrow$ PositionOfSibling(i)
  $\Phi_p \leftarrow$ Units(τ_p)
  $\Phi_s \leftarrow$ Units(τ_s)
  AdditiveTokens $\leftarrow \{+, -\}$
  MultiplicativeTokens $\leftarrow \{\times, /\}$
  PowerTokens $\leftarrow \{1/\square, \sqrt{\square}, \square^n\}$
  DimensionlessTokens $\leftarrow \{\cos, \sin, \tan, \exp, \log\}$
  if τ_p is in AdditiveTokens **and** Φ_s is known **then**
    $\Phi_i \leftarrow \Phi_s$
  else if τ_p is in AdditiveTokens **and** Φ_p is free **and** NodeRank(τ_i) is 2 **and** Φ_s is free **then**
    BottomUpUnitsAssignement(start $= s$, end $= i-1$)
    $\Phi_i \leftarrow \Phi_s$
  else if Φ_p is free **and** τ_p is **not** in MultiplicativeTokens **and** τ_s is **not** a placeholder **then**
    $\Phi_i \leftarrow$ free;
  else if $i = 0$ **then**
    $\Phi_i \leftarrow$ Units(root)
  else if τ_p is in AdditiveTokens **then**
    $\Phi_i \leftarrow \Phi_p$
  else if τ_p is in PowerTokens **then**
    $n \leftarrow$ Power(τ_p)
    $\Phi_i \leftarrow \Phi_p / n$
  else if $\Phi_p = \mathbf{0}$ **or** τ_p is in DimensionlessTokens **then**
    $\Phi_i \leftarrow \mathbf{0}$
  else if τ_p is in MultiplicativeTokens **then**
    if τ_i is a placeholder **and** τ_s is a placeholder **then**
      $\Phi_i \leftarrow$ free
    else if NodeRank(τ_i) is 1 **then**
      $\Phi_i \leftarrow$ free
    else if Φ_p is free **then**
      $\Phi_i \leftarrow$ free
    else
      BottomUpUnitsAssignement(start $= s$, end $= i-1$)
      if τ_i is $\{\times\}$ **then**
        $\Phi_i \leftarrow \Phi_p - \Phi_s$;
      else if τ_i is $\{/\}$ **then**
        $\Phi_i \leftarrow \Phi_s - \Phi_p$;
return Φ_i

is to generate these symbols according to fit quality and physical units constraints.

The training of the network that generates the distribution of symbols relies on the "reinforcement learning" strategy (Sutton & Barto 2018), which is a common method used to train artificial intelligence agents to navigate virtual worlds such as video games[3], or master open-ended tasks (Adaptive Agent Team et al. 2023). In the present context, the idea is to generate a set (usually called a "batch" in machine learning) of trial symbolic functions, and compute a scalar reward for each function by confronting it to the data. We can then require the neural network to generate a new batch of trial functions, encouraging it to produce better results by reinforcing behavior associated with high reward values, approximating gradients via a so-called "policy" (i.e., a quantitative strategy). The hope is that, by trial and error, the learnable parameters of the network will converge to values that are able to generate a symbolic function that fits the data well.

Following the insight by Petersen et al. (2019), we adopt the risk-seeking policy gradient along with the entropy regularization scheme found by Landajuela et al. (2021a). In essence, we only reinforce the best 5 % of candidate solutions, not penalizing the neural network for proposing the 95 % of other candidates, therefore maximizing the reward of the few best performing candidates rather than the average reward. This enables an efficient exploration of the search space at the expense of average performance, which is of particular interest in SR as we are only concerned in finding the very best candidates and do not care if the neural network performs well on average[4]. This novel risk-seeking policy, first proposed by Petersen et al. (2019), has significantly boosted performance in symbolic regression.

It is worth noting that our approach reinforces candidates which are sampled based on not only the output of the RNN, but also the local units constraints derived from the units prior distribution, which ensures the physical correctness of token choices. As a result, our approach effectively trains the RNN to make appropriate symbolic choices in accordance with local units constraints, in a quasi supervised learning manner. This combined with the general reinforcement learning paradigm enables us to produce both accurate and physically relevant symbolic expressions.

We allow the candidate functions f to also contain "constants" with fixed units, but with free numerical values. These free constants allow us the possibility to model situations where the problem has some unknown physical scales. A (somewhat contrived) example from

[3] See, e.g., `https://www.youtube.com/watch?v=QilHGSYbjDQ`

[4] This is contrary to many other applications of reinforcement learning (e.g., robotic automation, video games) which can even sometimes require risk-adverse gradient policies (e.g., self driving cars) (Rajeswaran et al. 2016).

galactic dynamics could be if we were provided a set of potential values Φ, and cylindrical coordinate values (R, z) of some mystery function that was actually a simple logarithmic potential model:

$$\Phi = \frac{1}{2} v_0^2 \ln \left(R_c^2 + R^2 + \frac{z^2}{q^2} \right), \tag{2}$$

whose parameters are the velocity parameter v_0, the core radius R_c and the potential flattening q. Of course, we will generally not know in advance either the number of such parameters that the correct solution requires, or their numerical values. Yet to be able to evaluate the loss of the trial functions f, we need to assign values to all such free "constants" they may contain. We accomplish this task by processing each trial function, with the L-BFGS (Zhu et al. 1997) optimization routine in *pytorch*, leveraging the fact that we can encode the symbols of f using *pytorch* functions. Since *pytorch* has in-built auto-differentiation, finding the optimal value of the constants via gradient descent is extremely efficient. However, due to the number of trial expressions to evaluate and considering that each expression must be evaluated multiple times to optimize its free constants, this optimization step is one of the main performance bottlenecks of the Φ-SO algorithm.

Then, as in Petersen et al. (2019) for each candidate f, we compute a reward R that is representative of fit quality: $R = 1/(1+\text{NRMSE})$ where NRMSE is the root mean squared error normalized by the deviation of the target σ_y: $\text{NRMSE} = \frac{1}{\sigma_y}\sqrt{\frac{1}{N}\sum_{i=1}^{N}(y_i - f(\mathbf{x}_i))^2}$. We apply the policy gradients by means of an Adam optimizer Kingma & Ba (2014) and use a long-short term memory (LSTM) type RNN (Hochreiter & Schmidhuber 1997). Our additional learning hyper-parameters can be found in Table 1. It is worth noting that the empirically tuned batch size we found (10k) is larger than the one found by Petersen et al. (2019) which was of 1k. We attribute this to the very strong constraints offered by our Φ-SO setup which require a strong exploration counterpart to avoid getting stuck in local minima.

It is also worth noting that in the reinforcement learning framework, the the reward function can be considered as as a black box, which does not have to be differentiable, therefore one could use anything as the reward. For example, we can also include the complexity of the symbolic function in the reward function, so as to have a criterion akin to Occam's razor. But actually one could in principle implement many ideas into the reward function: symmetries, constraints on primitives or derivatives, fitness in a differential equation, the results of some symbolic computation using external packages such as Mathematica (Wolfram 2003) or SymPy (Meurer et al. 2017), behavior of the function when implemented an n-body simulation, and so on.

Learning parameters	
Batch size	10 000
Learning rate	0.0025
Entropy coefficient	0.005
Risk factor	5 %

Table 1. Learning parameters.

4. CASE STUDIES

We showcase our Φ-SO method on a panel of astrophysical test cases: the relativistic energy of a particle is examined in subsection 4.1, the law describing the expansion of the Universe in subsection 4.2, the isochrone action from galactic dynamics in subsection 4.3 and additional toy test cases given in 4.4. These examples show that the method can successfully recover physical laws and relations from real or synthetic data. We limit ourselves to the exploration of 10 million trial expressions which roughly takes ~ 4 hours on a modern laptop computer and is only necessary for the most difficult case (the relativistic energy).

In addition, for some of these cases, we give the Pareto front which shows the most accurate expression based on RMSE (root mean squared error) for each level of complexity. Although we note that there are sophisticated schemes inspired by information theory to define the complexity (Udrescu & Tegmark 2020; Bartlett et al. 2022; Schmidt & Lipson 2009), we defer such considerations to a future study and simply define the complexity of each token to be of 1 except for input variables which we take to have complexity zero.

We also define the successful exact symbolic recovery of an expression by its symbolic equivalence using the SymPy symbolic simplification subroutine (Meurer et al. 2017) whenever possible and by a numerical criterion akin to the one used in (La Cava et al. 2021; Matsubara et al. 2022) $R > 0.9999$ along with manual verifications in cases where it is impossible to automatically simplify (e.g., when free constants are involved).

Finally, we agnostically rely on the same library of choosable tokens for all test cases: $\{+, -, \times, /, 1/\square, \sqrt{\square}, \square^2, \exp, \log, \cos, \sin, 1\}$ to which we only add input variables and free or fixed constants depending on the test cases.

4.1. *Relativistic energy of a particle*

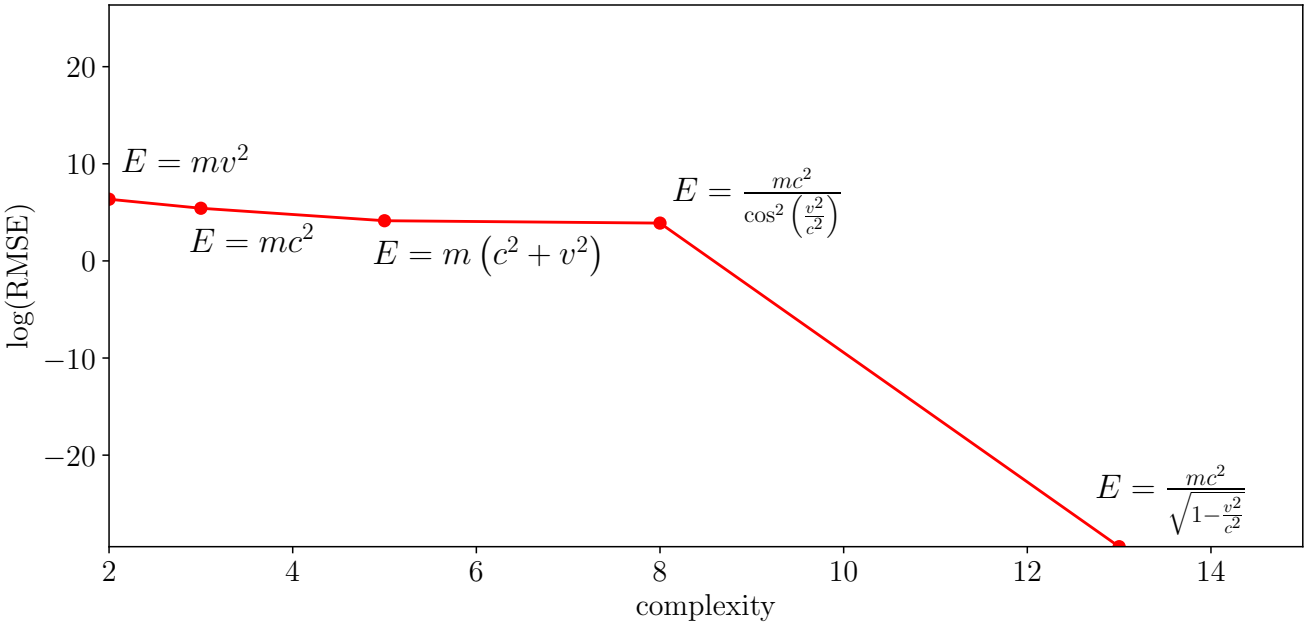

Figure 3. Pareto-front encoding accuracy-complexity trade off of recovered physical formulae typically recovered using our Φ-SO method when applied to data for the relativistic energy of a particle. We recover the relativistic expression as well as the classical approximation.

Let us consider the expression for the relativistic energy of a particle:

$$E = \frac{mc^2}{\sqrt{1 - \frac{v^2}{c^2}}}\,, \tag{3}$$

where m, v and c are respectively the mass of the particle, its velocity and the speed of light.

Using the aforementioned library of tokens as well as the $\{m, v\}$ input variables and a free constant $\{c\}$, Φ-SO is able to successfully recover this expression 100% of the time. Figure 3 contains the Pareto front of recovered expressions where similarly to Udrescu et al. (2020), we showcase that we are able to recover the relativistic energy of a particle as well as the classical approximation which has a lower complexity.

However, we note that contrary to the system proposed in (Udrescu et al. 2020) which mostly relies on powerful problem simplification schemes (in particular, the identification of symmetries as well as the identification of additive and multiplicative separability), our system is able to recover the exact expression for the relativistic energy test case without any simplification and without needing to simplify further the problem by treating c as a variable taking a range of different values as in (Udrescu et al. 2020). To the best of our knowledge our algorithm is the only one at present able to crack this case under these more stringent conditions.

4.2. *Expansion of the Universe*

The next case study we examine is the Hubble Diagram of supernovae type Ia, namely the change in the observed luminosity of these important standard candles as a function of redshift z. This is one of the major pieces of evidence that indicates that the Universe is experiencing an accelerating expansion, and it is also one of the observational pillars underlying Λ Cold Dark Matter (ΛCDM) cosmology in which Dark Energy dominates the energy-density budget of the Universe.

We will use the so-called *Pantheon* state-of-the-art compilation dataset (Scolnic et al. 2018), shown in Figure 4. We follow an almost identical methodology as Bartlett et al. (2022), to find the Hubble parameter $H(z)$ from the measured supernova magnitude and redshift pairs. Following Bartlett et al. (2022), we use the auxiliary function

$$y(x \equiv 1 + z) \equiv H(z)^2\,, \tag{4}$$

which for ΛCDM in a flat Universe with negligible radiation pressure is

$$y_{\Lambda\mathrm{CDM}}(x) = H_0^2(\Omega_m x^3 + (1 - \Omega_m))\,, \tag{5}$$

where Ω_m is the matter density parameter and H_0 is the Hubble constant. In this flat Universe model the

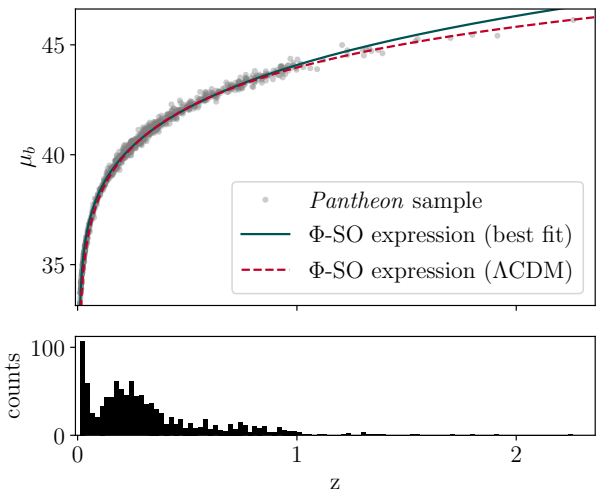

Figure 4. Symbolic regression results when applying the Φ-SO algorithm (allowing two free parameters) to the Hubble Diagram of supernovae Ia from the *Pantheon* sample. Φ-SO rediscovers the ΛCDM relation (in red) as well as another relation (in blue) which has a slightly better fit than ΛCDM when naively considering only *Pantheon*'s observational constraints due to the over-abundance of low z SNe.

cosmological luminosity distance is

$$d_L(z) = (1+z)\int_0^z \frac{c\,dz'}{H(z')}\,, \tag{6}$$

where c is the speed of light.

We adapt our machinery to the Hubble diagram problem by integrating numerically the $H(z) = \sqrt{y(z)}$ functions proposed by the algorithm under Eqn. 6 to obtain the implied luminosity distance d_L. These are then trivially converted into a distance modulus $\mu(z) = 5\log_{10}(d_L(z)/10\,\mathrm{pc})$, which can be compared to the *Pantheon* data.

This Hubble Diagram example showcases the capability of the software to include free "constants" (here we include one having the units of H_0 and the other being dimensionless as Ω_m) in the expression search, whose values are found thanks to auto-differentiation via L-BFGS optimization, as mentioned in Section 3.3. The optimal values of these constants need to be calculated after being passed through the numerical integration step (Eqn. 6), which turns out to be the main bottleneck of the problem in terms of computational cost. However, this also shows that the algorithm allows one to derive expressions that are subsequently passed through complicated operations before being compared to data.

Although we are able to successfully recover the ΛCDM expression given in equation 5 during the SR exploration using either synthetic data or the real *Pantheon* observational data, we note that as Bartlett et al. (2022), using observational data our system finds more accurate solutions at lower complexities than the ΛCDM model. We attribute that to the fact that our system is only given the chance to confront its trial model of $H(z)$ to a dataset of standard candles where there is an over abundance of low z events but not to other observational constraints such as the cosmic microwave background which might tilt the balance in favor of ΛCDM as the most accurate model at its level of complexity.

We note that contrary to the exhaustive symbolic regression approach proposed in Bartlett et al. (2022), we are able to recover this expression by typically exploring < 50k expressions (which takes a few minutes on a modern laptop) rather than 5×10^6 even given the fact that in this study we are allowing more functions $(\cos, \sin, \exp, \log)$, demonstrating the effectiveness of our approach.

4.3. *Isochrone action from galactic dynamics*

Another interesting application of symbolic regression is to derive perfect analytical properties of analytical models of physical systems. To this end, we chose to attempt to find the radial action J_r of the spherical isochrone potential.

$$\Phi(r) = -\frac{GM}{b+\sqrt{b^2+r^2}}\,, \tag{7}$$

where G is the gravitational constant, M is the mass of the model, b is a length scale of the model, and r is a spherical radius (Binney & Tremaine 2011). Action variables are special integrals of motion in integrable potentials which can be used to describe the orbit of an object in a system, and they are of particular interest in Galactic Archaeology as they are adiabatic invariants, so they are preserved if a galaxy or stellar system has evolved slowly. The isochrone is the only potential model to have actions known in analytic form in terms of elementary functions[5]. For the case of the isochrone model, the radial component of the action of a particle can be expressed as

$$J_r = \frac{GM}{\sqrt{-2E}} - \frac{1}{2}\left(L + \frac{1}{2}\sqrt{L^2 - 4GMb}\right), \tag{8}$$

where E and L are, respectively, the particle energy and total angular momentum (Binney & Tremaine 2011).

We provide our algorithm numerical values of J_r (which has units of angular momentum) given L and

[5] We have recently shown that actions can be calculated numerically from samples of points along orbits in realistic galaxy potentials using deep learning techniques (Ibata et al. 2021).

E, and leave b as a free scaling parameter. Since we expect each occurrence of M to be accompanied by an occurrence of the gravitational constant, we provide the algorithm with GM as a single variable.

This expression (Eqn. 8) could not be solved either by the standard DSR algorithm (Petersen et al. 2019), or by the AIFeynman algorithm (Udrescu & Tegmark 2020). Our algorithm was also not able to identify the equation in 10 million guesses. However, one of the steps of the AIFeynman algorithm is a test for additive and multiplicative separability of the mystery function, and it creates new datasets for each separable part. For the case of additive separability, the units remain unchanged, and so it is trivial to simply provide our Φ-SO algorithm these separated data to fit in turn, one at a time. Thus the first term of the right hand side of Eqn. 8 (with an E dependence) was easily solved together with a fitted additive free constant. We then subtracted the fitted constant from the second dataset, and Φ-SO correctly recovered the second term on the right hand side of Eqn. 8 (with an L dependence).

4.4. *Supplementary cases*

In addition to the cases above, we test our algorithm on a set of textbook equations. We include Newton's law of universal gravitation:

$$F = \frac{Gm_1m_2}{r^2}\,, \tag{9}$$

where G is the universal gravitational constant, m_1 and m_2 are the masses of the attracting bodies and r is the distance separating them. For this test case, we use $\{m_1, m_2, r\}$ as input variables and leave G as a free constant.

We also include a damped harmonic oscillator which appears in a wide range of (astro)-physical contexts:

$$y = e^{-\alpha t}\cos(ft + \Phi)\,, \tag{10}$$

where α and f are respectively the damping parameter and the frequency of oscillations (both homogeneous to the inverse of a time) and Φ is the (dimensionless) phase. We leave these three parameters as free constants and use t as our input variable.

Finally, we consider the Navarro–Frenk–White (NFW) profile (Navarro et al. 1996) which is an empirical relation that describes the density profile $\rho(r)$ of halos of collisionless dark matter in cosmological N-body simulations:

$$\rho = \frac{\rho_0}{\frac{r}{R_s}\left(1+\frac{r}{R_s}\right)^2}\,, \tag{11}$$

where r is the radius which we use as an input variable and ρ_0 and R_s are respectively the density and radius scale parameters which we leave as free constants.

5. RESULTS

In physics, we often seek to build approximate models, such as might be obtained via a polynomial function or a Fourier series fit to some data. In those instances, the root mean square error is usually the criterion of relevance to determine whether the procedure worked well or not. However, here we wish to recover the "true" underlying model, in which case the recovery rate should be the criterion of success.

The performance of Φ-SO on the test cases detailed above is summarized in the ablation study reported in Table 2. There we also report SR performance after disabling the units prior (only using the units informed RNN), disabling the RNN's ability to be informed of local units units constraints (only using the units prior and a standard SR RNN), disabling both the units prior and units information (only using a standard RNN which is equivalent to the Petersen et al. 2019 setup), doing a units guided random search by using a random number generator *in lieu* of the RNN, and finally doing a purely random search.

We show that merely constraining the choice of symbols using the external units prior distribution scheme (described in 3.2) is not enough to ensure perfect symbolic recovery of physical laws, but that informing the RNN of local units constraints (as described in 3.1) is essential as it allows the RNN to actively learn units rules. In addition, we show that our system does not only rely on a mere brute force approach combined with units constraints, but that the deep reinforcement learning setup described in 3.3 is an essential ingredient of the success of Φ-SO.

It should be noted that in the NFW test case, simply expressing the inverse of a third-degree polynomial is sufficient to solve the problem. However, using the units prior without enabling the RNN to observe local units constraints or utilizing the units prior in conjunction with a random number generator can result in a lower recovery rate compared to the use of a standalone random number generator. This is due to the highly restrictive nature of the units prior which in a simple case like this can actually slow down the convergence toward the solution.

Due to its very constraining nature, using a yet untrained RNN or a random number generator, our *in situ* units prior often conflicts with the length prior which is essential to avoid the expression generation phase going on forever. This typically results in the majority of expressions being discarded due to this conflict during the first epochs of training. However, enabling the RNN to learn on physically correct expressions, and enabling it able to observe local units constraints, allows it to ac-

Expression	# Trial expressions	Φ-SO ≡ {Φ-prior, Φ-RNN}	{Φ-RNN}	{Φ-prior, RNN}	{RNN}	{Φ-prior, RNG}	{RNG}
$E = \frac{mc^2}{\sqrt{1-v^2/c^2}}$	10M	100 %	0 %	60 %	0 %	20 %	0 %
$J_r = \frac{GM}{\sqrt{-2E}} - \frac{1}{2}\left(L + \frac{1}{2}\sqrt{L^2 - 4GMb}\right)$	4M	100 %	0 %	80 %	0 %	60 %	0 %
$\rho = \rho_0 / \left(\frac{r}{R_s}(1 + \frac{r}{R_s})^2\right)$	2M	100 %	100 %	40 %	100 %	20 %	100 %
$y = e^{-\alpha t}\cos(ft + \Phi)$	1M	100 %	0 %	0 %	0 %	0 %	0 %
$F = \frac{Gm_1m_2}{r^2}$	100K	100 %	80 %	100 %	20 %	80 %	0 %
$H^2(x \equiv 1+z) = {H_0}^2(\Omega_m x^3 + (1-\Omega_m))$	100K	100 %	100 %	100 %	100 %	40 %	40 %

Table 2. Exact symbolic recovery rate summary and ablation study on our panel of astrophysical examples (input variables and free parameters are colored in red and blue respectively). The acronymns are as follows. Φ-prior : physical units prior; Φ-RNN : physical units informed RNN; RNG : random number generator. By studying the performance in combinations of ablations of the *in situ* units prior, the RNN's ability to be informed of local units constraints, and of the RNN itself (i.e., replaced by a random number generator), we show that all three are essential ingredients of the success of our Φ-SO algorithm.

tively learn units rules as shown in Figure 5 which gives the fraction of physical expressions successfully generated over iterations of learning.

Finally, we also illustrate the generalization capabilities offered by virtue of finding the exact analytical expression compared to a good approximation in Figure 6, where we show that such analytical expressions can vastly outperform a multilayer perceptron (MLP) neural network.

6. DISCUSSION

Since the Deep Symbolic Regression framework (Petersen et al. 2019) and most other SR methods work by maximizing fit quality, there are few constraints on the arrangement of symbols. However, the paths in fit quality and the paths in symbol arrangement toward the global minima (perfect fit quality and perfect symbol arrangement) are not necessarily correlated. This results in the curse of accuracy guided SR, as small changes in fit quality can hide dramatic changes in functional form and vice-versa. In essence, one can improve fit quality of candidates over learning iterations while getting further away from the correct solution in symbolic arrangement. Therefore strong constraints on the functional form, such as the one we are proposing in our setup, are of great value for guiding SR algorithms in the context of physics. This is an advantage that physics has and that Φ-SO leverages by: (i) reducing the search space and (ii)

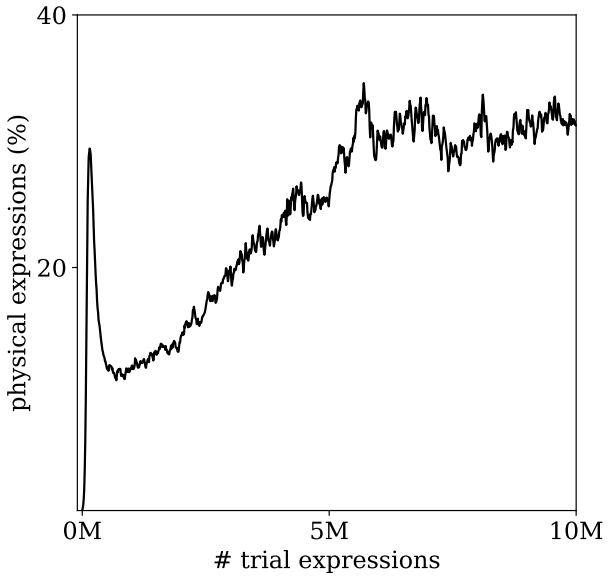

Figure 5. RNN learning units rules. The black line shows the evolution of the fraction of expressions that have balanced units. As the training progresses, the algorithm learns to respect the units constraints better. Here, we showcase this trend on the relativistic energy of a particle test case (averaged over multiple runs).

enabling the neural network to actively learn units rules and leverage them to explore the space of solutions more efficiently. Although the possibility of making a physical

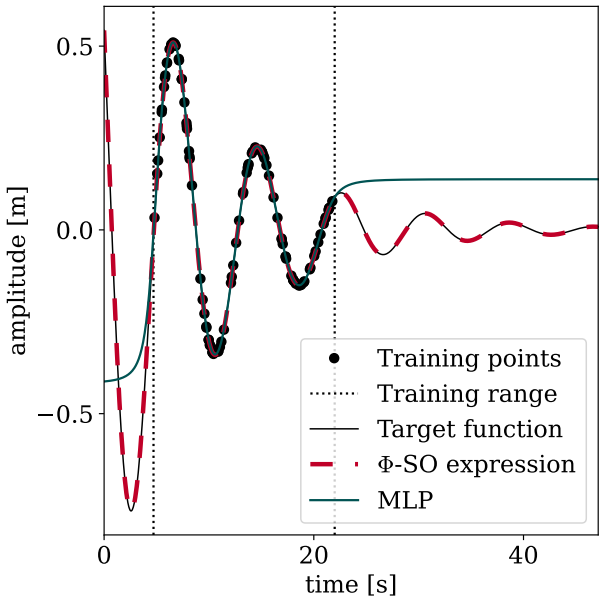

Figure 6. Example of the generalization capability of SR. Here we show randomly drawn data points (black dots) from a damped harmonic oscillator model (black line). The data are well fitted by an MLP (green line), which however fails in regions beyond the range of the training data (vertical dotted lines). In contrast, our SR algorithm Φ-SO (red dashed line) manages to provide much more reliable extrapolation.

units prior was hinted by Petersen et al. (2021), to the best of our knowledge such a framework was never built before.

For example, we note that in Wadekar et al. (2022), the relation is only in part generated by their genetic SR algorithm which is used to capture "a first order" approximation and that it had to be tinkered with by hand to make the expression physically meaningful and more accurate. We hope that our *in situ* units prior which can also be paired with alternative approaches will contribute to solving such issues.

The guidance offered by the units constraints gives Φ-SO an edge over other methods for finding the exact symbolic solutions, improving performance from a purely predictive standpoint. This makes Φ-SO a potentially useful tool for opening up black-box physics models such as neural networks fitted on data of physical phenomena. In addition, we note that in the context of physics, components of our Φ-SO framework can not only be used to improve the performance of algorithms built upon Petersen et al. (2019)'s framework (DiPietro & Zhu 2022; Du et al. 2022), but can also be used in tandem with other approaches. For instance, our *in situ* units prior can be used to reduce search space in the context of probabilistic or exhaustive searches (Bartlett et al. 2022; Kammerer et al. 2020; Brence et al. 2021; Jin et al. 2019), during the seeding phases of genetic algorithms (Schmidt & Lipson 2009; Cranmer 2020; Cranmer et al. 2020; Virgolin & Bosman 2022; Stephens 2015; Kommenda et al. 2020) or for making a physically motivated dataset of expressions, which in conjunction with enabling the RNN to be informed of local units constraints, could improve the performance of supervised end-to-end approaches (Kamienny et al. 2022; Vastl et al. 2022; Becker et al. 2022; Biggio et al. 2020).

Our approach is based on a deep reinforcement learning methodology, where the neural network is reinitialized at the start of each SR task. It is therefore trained independently for each specific problem, and so does not benefit from past experience nor is it pre-trained on a dataset of well known physical functional forms. One could argue that this makes our approach "unbiased" akin to unsupervised learning setups and therefore well suited for discovering new physics (Karagiorgi et al. 2022). However, this also intrinsically limits SR capabilities as exploiting such prior knowledge is of great value for resolving the curse of accuracy guided SR described above. One can exploit such prior knowledge by formulating it as an *in situ* prior (Kim et al. 2021) or by learning on it in a supervised manner using transformers learning techniques (Kamienny et al. 2022; Vastl et al. 2022). However, although state-of-the-art supervised SR methods, as of now, shine in providing accurate approximations, they show poorer exact symbolic expression recovery rates than other methods. Future work attempting to incorporate supervised learning with reinforcement learning as in Fan et al. (2022), so as to map the relationship between data points and mathematical expressions, may allow the recovery of expressions of substantially greater complexity than those we have explored in Section 4.

As we have shown in Section 4.3, it is straightforward to improve our method by combining it with the powerful problem simplification schemes devised in (Udrescu & Tegmark 2020; Udrescu et al. 2020; Luo et al. 2017; Tohme et al. 2022; Cranmer et al. 2020). The results of the separability procedures implemented in the (Udrescu et al. 2020) algorithm are conveniently recorded in separate datafiles, which makes it completely straightforward to use their approach as a pre-processing step for Φ-SO. We expect that it will be relatively easy to reproduce their method inside our algorithm which should lead to improved performances for Φ-SO.

It could be argued that we could have tackled the physical units validity of expressions in SR by using the Buckingham Π theorem (Buckingham 1914), with vari-

ables and constants rendered dimensionless by means of multiplicative operations amongst them (such an approach has recently been proposed by Matchev et al. 2022; Keren et al. 2023). However, working on so called Π groups can make SR much more difficult in practice as it makes the dimensionless solutions often more complex. It is interesting to note that nature (or at least physics) is not dimensionless, so information is lost during the process of making variables and constants dimensionless. This would have prevented us from leveraging the powerful constraints provided by the units.

7. CONCLUSIONS

We have presented a new symbolic regression algorithm, built from the ground up to make use of the highly restrictive constraint that we have in the physical sciences that our equations must have balanced units. The heart of the algorithm is an embedding that generates a sequence of mathematical symbols while cumulatively keeping track of their physical units. We adopt the very successful deep reinforcement learning strategy of Petersen et al. (2019), which we use to train our RNN to not only produce accurate expressions but physically sound ones by making it learn local units constraints.

The algorithm was applied to several test cases from astrophysics. The first was a simple search for the energy of a particle in Special Relativity (Section 4.1), which our algorithm was easily able to find, yet is a problem that the standard Petersen et al. (2019) code fails on. The second test case applied the algorithm to the famous Hubble diagram of supernovae of type Ia. While the form of the Hubble parameter $H(z)$ in standard ΛCDM cosmology was indeed recovered, the algorithm finds that other simpler solutions fit the supernova data (in isolation) better. This result is consistent with the findings of Bartlett et al. (2022). Another test examined a relatively complicated function in galactic dynamics, where we searched for the functional form of the radial action coordinate in an isochrone stellar potential model. Although our algorithm initially fails in this test, we managed to recover the correct equation by first splitting the dataset using the additive separability criterion as implemented by Udrescu & Tegmark (2020). No algorithm other than Φ-SO was able to recover this equation.

These tests have demonstrated the applicability of the algorithm to model data of the real world as well as to derive non-obvious analytic expressions for properties of perfect mathematical models of physical systems. Although we realise that the physical laws potentially discovered by our method will depend on data range, choice of priors, etc, this is a step toward a full agnostic method for connecting observational data to theory. Future contributions in this research program will extend the algorithm to allow for differential and integral operators, potentially permitting the solution of ordinary and partial differential equations with physical units constraints. However, our primary goal will be to use the new machinery to discover as yet unknown physical relationships from the state-of-the-art large surveys that the community has at its disposal.

CODE AVAILABILITY

The documented code for the Φ-SO algorithm along with demonstration notebooks are available on GitHub github.com/WassimTenachi/PhySO.

ACKNOWLEDGMENTS

RI acknowledges funding from the European Research Council (ERC) under the European Unions Horizon 2020 research and innovation programme (grant agreement No. 834148).

REFERENCES

117th US Congress. 2022, Algorithmic Accountability Act. https://www.congress.gov/bill/117th-congress/house-bill/6580/

Adaptive Agent Team, Bauer, J., Baumli, K., et al. 2023, arXiv e-prints, arXiv:2301.07608, doi: 10.48550/arXiv.2301.07608

Alnuqaydan, A., Gleyzer, S., & Prosper, H. 2022, Machine Learning: Science and Technology

Aréchiga, N., Chen, F., Chen, Y.-Y., et al. 2021, arXiv preprint arXiv:2112.04023

Arrieta, A. B., Díaz-Rodríguez, N., Del Ser, J., et al. 2020, Information fusion, 58, 82

Bartlett, D. J., Desmond, H., & Ferreira, P. G. 2022, arXiv preprint arXiv:2211.11461

Becker, S., Klein, M., Neitz, A., Parascandolo, G., & Kilbertus, N. 2022, arXiv preprint arXiv:2211.02830

Biggio, L., Bendinelli, T., Lucchi, A., & Parascandolo, G. 2020, in Learning Meets Combinatorial Algorithms at NeurIPS2020

Binney, J., & Tremaine, S. 2011, Galactic dynamics, Vol. 13 (Princeton university press)

Brence, J., Todorovski, L., & Džeroski, S. 2021, Knowledge-Based Systems, 224, 107077

Buckingham, E. 1914, Physical review, 4, 345

Carilli, C., & Rawlings, S. 2004, arXiv preprint astro-ph/0409274

Cranmer, M. 2020, PySR: Fast & Parallelized Symbolic Regression in Python/Julia, Zenodo, doi: 10.5281/zenodo.4041459

Cranmer, M., Sanchez Gonzalez, A., Battaglia, P., et al. 2020, Advances in Neural Information Processing Systems, 33, 17429

d'Ascoli, S., Kamienny, P.-A., Lample, G., & Charton, F. 2022, arXiv preprint arXiv:2201.04600

Delgado, A. M., Wadekar, D., Hadzhiyska, B., et al. 2022, Monthly Notices of the Royal Astronomical Society, 515, 2733

Desmond, H., Bartlett, D. J., & Ferreira, P. G. 2023, arXiv preprint arXiv:2301.04368

DiPietro, D. M., & Zhu, B. 2022, arXiv preprint arXiv:2209.01521

Du, M., Chen, Y., & Zhang, D. 2022, arXiv preprint arXiv:2210.02181

European Commission. 2021, The Artificial Intelligence Act. https://artificialintelligenceact.eu/

Fan, L., Wang, G., Jiang, Y., et al. 2022, arXiv preprint arXiv:2206.08853

Gaia Collaboration, Prusti, T., de Bruijne, J. H. J., et al. 2016, A&A, 595, A1, doi: 10.1051/0004-6361/201629272

Galilei, G. 1623, Il saggiatore

Graham, M. J., Djorgovski, S., Mahabal, A. A., Donalek, C., & Drake, A. J. 2013, Monthly Notices of the Royal Astronomical Society, 431, 2371

Hochreiter, S., & Schmidhuber, J. 1997, Neural computation, 9, 1735

Ibata, R., Diakogiannis, F. I., Famaey, B., & Monari, G. 2021, ApJ, 915, 5, doi: 10.3847/1538-4357/abfda9

Ivezić, Ž., Kahn, S. M., Tyson, J. A., et al. 2019, ApJ, 873, 111, doi: 10.3847/1538-4357/ab042c

Jin, Y., Fu, W., Kang, J., Guo, J., & Guo, J. 2019, arXiv preprint arXiv:1910.08892

Kamienny, P.-A., d'Ascoli, S., Lample, G., & Charton, F. 2022, arXiv preprint arXiv:2204.10532

Kammerer, L., Kronberger, G., Burlacu, B., et al. 2020, in Genetic Programming Theory and Practice XVII (Springer), 79–99

Karagiorgi, G., Kasieczka, G., Kravitz, S., Nachman, B., & Shih, D. 2022, Nature Reviews Physics, 4, 399

Keren, L. S., Liberzon, A., & Lazebnik, T. 2023, Scientific Reports, 13, 1249, doi: 10.1038/s41598-023-28328-2

Kim, J. T., Landajuela, M., & Petersen, B. K. 2021, arXiv preprint arXiv:2104.05930

Kim, S., Lu, P. Y., Mukherjee, S., et al. 2020, IEEE transactions on neural networks and learning systems, 32, 4166

Kingma, D. P., & Ba, J. 2014, arXiv preprint arXiv:1412.6980

Kommenda, M., Burlacu, B., Kronberger, G., & Affenzeller, M. 2020, Genetic Programming and Evolvable Machines, 21, 471

La Cava, W., Orzechowski, P., Burlacu, B., et al. 2021, arXiv preprint arXiv:2107.14351

Landajuela, M., Petersen, B. K., Kim, S. K., et al. 2021a, arXiv preprint arXiv:2107.09158

—. 2021b, arXiv preprint arXiv:2107.09158

Laureijs, R., Amiaux, J., Arduini, S., et al. 2011, arXiv e-prints, arXiv:1110.3193. https://arxiv.org/abs/1110.3193

Lemos, P., Jeffrey, N., Cranmer, M., Ho, S., & Battaglia, P. 2022, arXiv preprint arXiv:2202.02306

Liu, Z., & Tegmark, M. 2021, Physical Review Letters, 126, 180604

Liu, Z., Wang, B., Meng, Q., et al. 2021, Physical Review E, 104, 055302

LSST Science Collaboration, Abell, P. A., Allison, J., et al. 2009, arXiv e-prints, arXiv:0912.0201. https://arxiv.org/abs/0912.0201

Lu, Z., Pu, H., Wang, F., Hu, Z., & Wang, L. 2017, Advances in neural information processing systems, 30

Luo, C., Chen, C., & Jiang, Z. 2017, arXiv preprint arXiv:1705.08061

Makke, N., & Chawla, S. 2022, arXiv preprint arXiv:2211.10873

Martius, G., & Lampert, C. H. 2016, arXiv preprint arXiv:1610.02995

Matchev, K. T., Matcheva, K., & Roman, A. 2022, The Astrophysical Journal, 930, 33

Matsubara, Y., Chiba, N., Igarashi, R., & Ushiku, Y. 2022, in NeurIPS 2022 AI for Science: Progress and Promises. https://openreview.net/forum?id=oKwyEqClqkb

McConaghy, T. 2011, in Genetic Programming Theory and Practice IX (Springer), 235–260

Meurer, A., Smith, C. P., Paprocki, M., et al. 2017, PeerJ Computer Science, 3, e103

Murdoch, W. J., Singh, C., Kumbier, K., Abbasi-Asl, R., & Yu, B. 2019, Proceedings of the National Academy of Sciences, 116, 22071

Navarro, J. F., Frenk, C. S., & White, S. D. M. 1996, ApJ, 462, 563, doi: 10.1086/177173

Panju, M., & Ghodsi, A. 2020, arXiv preprint arXiv:2011.02415

Paszke, A., Gross, S., Massa, F., et al. 2019, Advances in neural information processing systems, 32

Petersen, B. K., Larma, M. L., Mundhenk, T. N., et al. 2019, arXiv preprint arXiv:1912.04871

Petersen, B. K., Santiago, C. P., & Landajuela, M. 2021, arXiv preprint arXiv:2107.09182

Press, W. H., Teukolsky, S. A., Vetterling, W. T., & Flannery, B. P. 2007, Numerical recipes 3rd edition: The art of scientific computing (Cambridge university press)

Rajeswaran, A., Ghotra, S., Ravindran, B., & Levine, S. 2016, arXiv preprint arXiv:1610.01283

Reinbold, P. A., Kageorge, L. M., Schatz, M. F., & Grigoriev, R. O. 2021, Nature communications, 12, 1

Sabbatini, F., & Calegari, R. 2022, arXiv preprint arXiv:2211.00238

Sahoo, S., Lampert, C., & Martius, G. 2018, in International Conference on Machine Learning, PMLR, 4442–4450

Schmidt, M., & Lipson, H. 2009, science, 324, 81

Scolnic, D. M., Jones, D. O., Rest, A., et al. 2018, ApJ, 859, 101, doi: 10.3847/1538-4357/aab9bb

Shao, H., Villaescusa-Navarro, F., Genel, S., et al. 2022, The Astrophysical Journal, 927, 85

Stephens, T. 2015, GPLearn. https://gplearn.readthedocs.io/en/stable/index.html

Sutton, R. S., & Barto, A. G. 2018, Reinforcement learning: An introduction (MIT press)

Tohme, T., Liu, D., & Youcef-Toumi, K. 2022, arXiv preprint arXiv:2205.15569

Udrescu, S.-M., Tan, A., Feng, J., et al. 2020, Advances in Neural Information Processing Systems, 33, 4860

Udrescu, S.-M., & Tegmark, M. 2020, Science Advances, 6, eaay2631

Usama, M., & Lee, I.-Y. 2022, Sensors, 22, 8240

Valle, C. M. C., & Haddadin, S. 2021, arXiv preprint arXiv:2105.14396

Vastl, M., Kulhánek, J., Kubalík, J., Derner, E., & Babuška, R. 2022, arXiv preprint arXiv:2205.15764

Virgolin, M., & Bosman, P. A. 2022, arXiv preprint arXiv:2204.12159

Virgolin, M., & Pissis, S. P. 2022, arXiv preprint arXiv:2207.01018

Wadekar, D., Villaescusa-Navarro, F., Ho, S., & Perreault-Levasseur, L. 2020, arXiv preprint arXiv:2012.00111

Wadekar, D., Thiele, L., Villaescusa-Navarro, F., et al. 2022, arXiv preprint arXiv:2201.01305

Wilstrup, C., & Kasak, J. 2021, arXiv preprint arXiv:2103.15147

Wolfram, S. 2003, The mathematica book, Vol. 1 (Wolfram Research, Inc.)

Wong, K. W., & Cranmer, M. 2022, arXiv preprint arXiv:2207.12409

Wu, T., & Tegmark, M. 2019, Physical Review E, 100, 033311

Zheng, W., Sharan, S., Fan, Z., et al. 2022, arXiv preprint arXiv:2212.14849

Zhu, C., Byrd, R. H., Lu, P., & Nocedal, J. 1997, ACM Transactions on mathematical software (TOMS), 23, 550